

## Liquid Properties of Embryonic Tissues: Measurement of Interfacial Tensions

Ramsey A. Foty,<sup>1</sup> Gabor Forgacs,<sup>2</sup> Cathie M. Pflieger,<sup>1</sup> and Malcolm S. Steinberg<sup>1,\*</sup>

<sup>1</sup>*Department of Molecular Biology, Princeton University, Princeton, New Jersey 08544*

<sup>2</sup>*Department of Physics, Clarkson University, Potsdam, New York 13699-5820*

(Received 23 November 1993)

The flow of embryonic tissues during morphogenesis has been ascribed to tissue interfacial tensions arising from cell adhesion. Testing this explanation requires the demonstration that tissue interfacial tensions are measurable physical quantities. We describe a device that continuously records all parameters necessary to determine the tensions of living tissues at the interface with the surrounding medium. We monitor the relaxation of an imposed stress in two embryonic tissues, measure their interfacial tensions, and demonstrate that these are consistent with these tissues' mutual spreading behavior.

PACS numbers: 87.45.Bp, 68.10.Cr, 68.10.Gw

We explore in this work the similarity between the behavior of immiscible liquids and that of embryonic tissues (reviewed in [1]). A droplet of the oil *n*-octanol will spread over the surface of a droplet of water, enveloping it completely. If the two droplets, instead of being opposed, are codispersed, the two kinds of molecules undergo phase separation, the water molecules forming a discontinuous phase of coalescing smaller droplets enveloped by a continuous phase of oil. In the absence of gravity, a spherical drop of water enveloped by oil is the minimal free energy or equilibrium configuration for this combination of liquids; the same configuration arrived at by spreading in the former case. Miscibility, immiscibility, phase separation, mutual spreading of contacting droplets, the process by which these rearrangements progress, and the configuration finally adopted are all determined by the interfacial tensions at the boundaries of the contacting phases.

Let  $\sigma_a$ ,  $\sigma_b$ , and  $\sigma_{ab}$  represent, respectively, the surface tensions of liquid phases *a* and *b* in an ambient medium and the interfacial tension between these two phases. Phases *a* and *b* will be immiscible if  $\sigma_{ab} > 0$ . If, in addition,  $\sigma_a > \sigma_b$ , phase *b* will spread over the surface of phase *a*. The above relationship makes it clear that, among mutually immiscible phases, the tendency of one to spread upon another must be transitive: That is, if *a* is spread upon by *b* and *b* is spread upon by *c*, then *a* will be spread upon by *c*. Moreover, if  $\sigma_a > (\sigma_a + \sigma_b - \sigma_{ab})/2 \geq \sigma_b$ , envelopment of *a* by *b* will be complete rather than partial [2].

All of the liquid behaviors described above have been demonstrated to be displayed by tissues of vertebrate embryos. For example, in tissue culture, a fragment of embryonic epidermis will spread over and envelop a fragment of future embryonic brain tissue. Also, embryonic epidermal cells and future brain cells, when dissociated and mixed together, "sort out" from one another [3]. Where the time course of such cell sorting has been observed, it has been seen to progress by a process of coalescence [4-6] (note also Figs. 16 and 17 in [3]). The same configuration is approached through cell sorting as through tissue spreading [7,8]. When a number of embryonic tissues were paired in all possible binary com-

binations, it was found that their mutual envelopment tendencies form a transitive series [8]. These liquidlike behaviors are not confined to a few kinds of embryonic tissues. Rather, they are properties common among embryonic tissues, especially during the earlier stages of development, when isolated, irregular tissue fragments smooth out their irregularities, often rounding up to form spheroids, a hallmark of the liquid state. Moreover, when the component tissues or cells of a particular organ or other body structure are isolated and recombined *in vitro*, the organization they tend to adopt is similar to the normal one [3,9]. The spreading of one tissue over the surface of another is a common means of normal embryonic morphogenesis [10,11]. We have concluded that the properties responsible for liquid tissue behavior are utilized by embryos to guide the assembly of their cells and tissues into anatomically "correct" higher level structures (see Ref. [1]). For a thorough review of this subject, see [6].

A liquid can be regarded as a population of mobile, cohesive subunits. Many behaviors of liquids depend not at all upon the identities of the subunits (e.g., molecules vs cells) or the reasons why they are either mobile or cohesive but only upon their being describable in these terms. Tissue cells cohere because their surfaces display molecules specialized for adhesion. They utilize molecular machinery that enables them to move about [12]. Thus a population of such living cells has certain qualities of a liquid. Cell aggregates round up to form a sphere or spread upon a substratum to form a monolayer. The *differential adhesion hypothesis* (reviewed in [1,6]) traces the liquidlike rounding, spreading, and segregating behavior of motile cell populations to interfacial free energies arising from cellular adhesive interactions. The anatomical structure approached through such cell rearrangements would represent an equilibrium configuration in which the interfacial free energy of the system is minimized. Important elements of animal form and structure would therefore be encoded through specification of cells' adhesive properties, which would in turn generate corresponding tensions at tissue surfaces and interfaces. Both biological cell sorting and the engulfment of one tissue mass by another, driven by differential adhesion, have re-

cently been simulated very accurately in two dimensions using the extended two-dimensional large- $Q$  Potts model [13,14].

Testing the differential adhesion hypothesis (and with it the possible relevance of interfacial phenomena to morphogenesis [15]) requires measurement of the interfacial tensions it invokes to explain tissue spreading and cell sorting behavior. Some standard methods for the measurement of surface and interfacial tensions (the du Noüy ring method, the pendant drop method) are unsuitable for application to living cell aggregates, which must be kept within narrow size limits, at which they are little distorted by gravity, which have very high viscosity [16], and which must remain in good health during the measurement. In our first efforts to measure embryonic tissue interfacial tensions, we employed the sessile drop method. It required forces on the order of (4000–8000) $g$ , applied to the cell aggregates in a specially designed incubator and centrifuge, to flatten them significantly. The resulting data enabled us to rank the surface tensions of chick

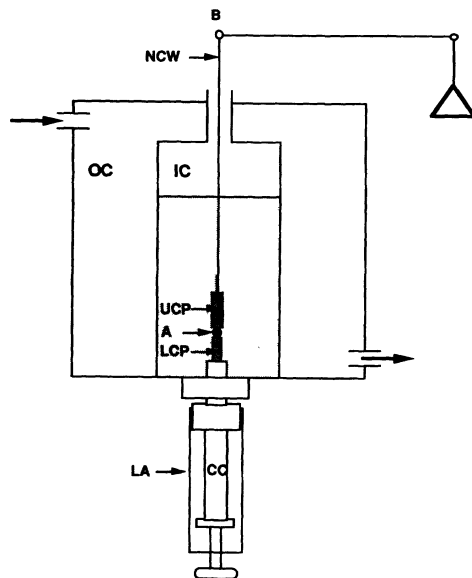


FIG. 1. The parallel plate compression apparatus (not drawn to scale) contains inner and outer Plexiglas chambers. The outer chamber (OC) is connected to a thermostated circulating water pump and serves to maintain the temperature of the inner chamber (IC), which contains tissue culture medium. The lower assembly (LA) screws into the base of the inner chamber, sealing its bottom. The position of its central core (CC), whose tip is the lower compression plate (LCP), can be adjusted vertically to set the distance between the two plates. The upper compression plate (UCP) is a cylinder about 15 mm long suspended from the balance arm (B) by a 0.15 mm diameter nickel-chromium wire (NCW). Its position can be adjusted horizontally to place the upper plate above the aggregate. During an experiment, the cell aggregate (A) is positioned on the lower plate and raised until it contacts the upper plate. Compression of the aggregate reduces the load measured by the balance by an amount equal to the force acting upon the cell aggregate.

embryonic limb bud, heart ventricle, and liver aggregates as declining in the order stated, in agreement with the mutual spreading behavior of these tissues [17]. However, numerical values of these tissue interfacial tensions were not obtained.

In this Letter, we introduce a thermostated parallel plate compression apparatus specifically designed to evaluate the aggregate and medium interfacial tensions of living cell aggregates. This is done through continuous recordings of both force and shape, enabling the approach to shape equilibrium to be constantly monitored. Using this instrument, we demonstrate the compound course of stress relaxation within compressed aggregates. We report the values obtained for chick embryonic heart ventricle and liver aggregate interfacial tensions and show that these values are area invariant and correlate with earlier results of tissue spreading and cell sorting experiments.

The apparatus used in this work is represented schematically in Fig. 1. The living tissues used for the measurements were obtained from 5 to 6 day old chick embryos. Their cells were dissociated in a solution of the proteolytic enzyme trypsin and allowed to form aggregates in a tissue culture medium, following procedures similar to those used previously [17]. When cultured in a 37°C shaker bath for about a day, these aggregates adopted an almost perfect spherical shape. To initiate a measurement, the inner chamber of the apparatus was filled with prewarmed tissue culture medium and a spherical aggregate ranging in diameter from about 200  $\mu\text{m}$  to about 500  $\mu\text{m}$  (containing on the order of  $10^4$  cells) was positioned on the lower compression plate [LCP; Figs. 1 and 2(a)]. The upper compression plate (UCP) was suspended from the balance arm and recording of its apparent weight was begun, establishing the precompression zero force baseline. The UCP was centered above the LCP, which was then raised until the aggregate was compressed between the two [Fig. 2(b)]. Different degrees of compression were achieved by adjusting the height of the LCP. The aggregate's profile was continuously recorded with a time lapse video cassette recorder connected to a video camera coupled to a horizontal Wild model M-5 stereomicroscope using 50 $\times$  magnification. Changes in the force exerted by the aggregate upon the UCP were continuously measured by a Cahn/Ventron (Cerritos, CA) model C-2000 recording electrobalance and recorded on a strip chart recorder. Achievement of

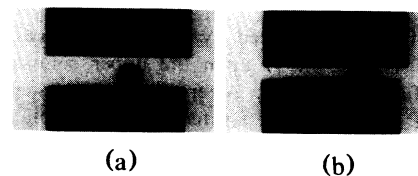


FIG. 2. (a) Spherical liver aggregate on lower compression plate before compression. (b) Same aggregate after initiation of compression.

shape equilibrium was denoted by the leveling off of the force reading [Fig. 3(a)] and confirmed by observation of the cessation of aggregate shape change.

Following application of a compressing force, relaxation was found to be biphasic. A significant fraction of the induced stress was dissipated within a few minutes in all cases. However, maximal relaxation usually took an hour or two for liver aggregates [Fig. 3(a)] and about eight hours for heart aggregates (data not shown). This is in accord with the earlier characterization of such cell aggregates, in centrifugation studies, as elasticoviscous liquids. The rapid, elastic response to the application of a distorting force was found to be associated with cell deformations, these being reversed in the course of the longer-term cell rearrangements that accompanied the approach to shape equilibrium [18,19].

The surface tension of a liquid droplet compressed between parallel plates to which it does not adhere can be obtained from the Laplace equation [20]

$$\sigma(1/R_1 + 1/R_2) + P_{ext} = \lambda. \tag{1}$$

Here  $P_{ext}$  is the external pressure acting on the droplet's surface,  $\sigma$  is the interfacial pressure between the droplet and the immersion medium, and  $R_1$  and  $R_2$  are the two principal radii of curvature of the droplet's surface (Fig. 4). In Eq. (1),  $\lambda$  is a constant Lagrange multiplier assuring the incompressibility (constant volume) of the aggregate. Equation (1) in general implies a local relationship at any given point on the boundary of the aggregate and, as such, represents a complicated partial differential

equation. If, however, the aggregate is spherical prior to compression, as is approximately the case [see Fig. 2(a)], it will be axially symmetric after compression (at equilibrium). Furthermore, we approximate the side boundaries of the aggregate by spherical caps. Then, evaluating Eq. (1) along the upper or lower compression plates (we neglect gravity), we obtain  $\lambda = F/\pi R_3^2$ , where the expression on the right hand side is the external pressure due to compression,  $F$  is the measured weight loss of the UCP in dynes, and  $R_3$  the radius shown in Fig. 4. Once  $\lambda$  is known, Eq. (1) can be evaluated at point  $O$  (see Fig. 4) along the side boundary of the aggregate (where  $P_{ext} = 0$ ), with the result

$$\sigma = \frac{F}{\pi R_3^2} \left( \frac{1}{R_1} + \frac{1}{R_2} \right)^{-1}. \tag{2}$$

Videorecorded aggregate profile images, representing equilibrium shapes, were digitized, converted to eight bit gray scale files, and transferred to a Mac Centris 650 8/230 computer for analysis. Using NIH Image software, circles of adjustable radii were superimposed upon and matched to the images of the aggregate's sides [Fig. 3(b)]. Very good congruence was obtained. A linear tracing function was then used to measure  $R_1$ ,  $R_2$ , and  $R_3$ . In each case, four  $\sigma$  values were calculated, using  $R_2$  taken from the aggregate's left and right sides and  $R_3$  taken from its upper and lower surfaces. These four values were then averaged.

The results for three representative liver aggregates and three representative heart ventricle aggregates are shown in Table I. The greatest deviation from the mean value was 10% in the liver group and 4% in the heart group. An essential requirement for our analysis is that these interfacial tensions be area invariant, characteristic of liquid rather than of solid bodies. This means that distinct sets of the quantities  $F$ ,  $R_1$ ,  $R_2$ , and  $R_3$  measured on the same aggregate at different degrees of compression should yield the same value of  $\sigma$ . We verified this by subjecting the same aggregate to two successive compressions, the second greater than the first [Figs. 3(a) and 3(b)]. As shown in Table I, the values thus obtained are consistent with the requirement for area invariance. The results, 8.3 dyn/cm for heart ventricle and 4.3 dyn/cm for liver, confirm the qualitative relationship  $\sigma_{heart} > \sigma_{liver}$  ob-

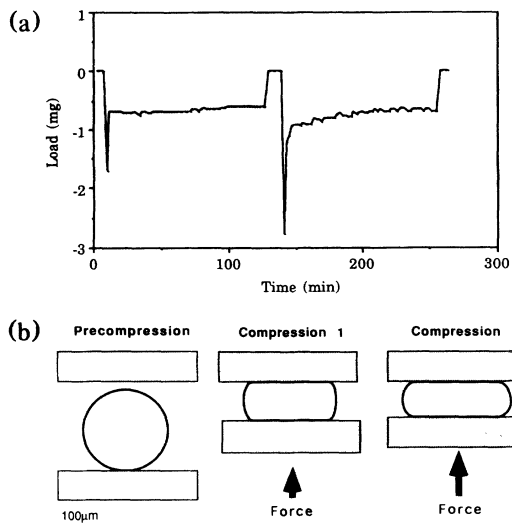


FIG. 3. (a) Force exerted by initially spherical chick liver aggregate 1 (see Table I) upon the upper compression plate (load) as a function of time. After relaxation was complete, the compressing plates were separated and the equilibrium force determined. A second, greater compression was then initiated and the process was repeated. (b) Profile shapes of chick liver aggregate 1, traced using NIH Image are shown before compression was initiated and immediately preceding termination of each compression.

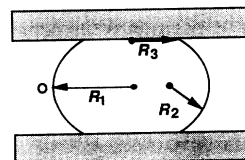


FIG. 4. A liquid droplet compressed between parallel plates to which it does not adhere, at shape equilibrium.  $R_1$  and  $R_2$  are the two primary radii of curvature, respectively, in the plane of and normal to the droplet's axis of symmetry.  $R_3$  is the radius of the droplet's circular area of contact with either compression plate.

TABLE I. Aggregate and medium interfacial tensions of cell aggregates of embryonic chick liver and heart ventricle. Whenever the same aggregate was subjected to two successive compressions, the second greater than the first, the two  $\sigma$  values obtained are listed in the order in which they were measured.

Cell aggregate	$\sigma$ (dyn/cm)	Mean $\sigma \pm$ S.E.
Liver 1	4.3	
	4.6	
Liver 2	4.4	Liver
Liver 3	4.2	$4.3 \pm 0.1$
	3.9	
Heart 1	8.4	
	8.5	Heart
Heart 2	8.0	$8.3 \pm 0.1$
Heart 3	8.3	

tained previously [17] and required to explain the engulfment of embryonic heart ventricle by liver cell populations [1,7,8].

The following remarks are due concerning these measurements. (1) As a test of the accuracy of our instrument, we measured the surface tension of the culture medium by compressing an air bubble in our device ( $\sigma = 39$  dyn/cm) and by the de Noüy ring method ( $\sigma = 42$  dyn/cm). (2) To minimize adherence of cell aggregates to the compression plates, both the lower and upper plates were coated before each use with poly(2-hydroxyethyl-methacrylate) [poly(HEMA)], a polymeric material to which cells adhere very poorly [21]. (3) Only measurements on cell aggregates with smooth contours at the end of a compression were used. (4) In the case of heart aggregates,  $10^{-4}M$  verapamil, a blocker of the slow calcium channel, was included in the medium to prevent them from beating [22].

In conclusion, by direct measurements we have here confirmed and quantified, to our knowledge for the first time, the biphasic relaxation of stress in certain embryonic cell aggregates in response to a deforming force. We demonstrate that such aggregates display tissue-specific, area-invariant interfacial tensions, consistent with liquidity. We measure these interfacial tensions using aggregates of chick embryonic heart ventricle and liver cells. We show that their tensions fall in the sequence required to account for the mutual envelopment properties of these two tissues. This is in accord with the findings of an earlier parallel plate compression study of amphibian embryonic ectoderm, mesoderm, and endoderm in which tissue envelopment behavior was also correlated with measurements of tissue interfacial tensions [23,24]. All of these results support the hypothesis that such "morphogenetic movements" are guided by tissue interfacial tensions generated by adhesive interactions among and between the migrating cells and their embryonic substrata.

R.A.F. was a recipient of a postdoctoral fellowship from the Natural Sciences and Engineering Research

Council of Canada. G.F. was supported by NSF Grant No. IBN 93-17633 and also benefited from the financial support of the Princeton Materials Institute during his stay at Princeton University. We acknowledge the contribution of Eric J. Olson to the early development and testing of our tissue surface tensiometer [25] and the technical assistance of Edward Kennedy. This work was supported by research Grant No. HD30345 from the NICHD, National Institutes of Health.

\*To whom correspondence should be addressed.

- [1] M. S. Steinberg, in *Dynamical Phenomena at Interfaces, Surfaces and Membranes*, edited by D. Beysens, N. Boccara, and G. Forgacs (Nova Science Publishers, Commack, NY, 1993), p. 3.
- [2] J. T. Davies and E. K. Rideal, *Interfacial Phenomena* (Academic, New York, 1963).
- [3] P. L. Townes and J. Holtfreter, *J. Exptl. Zool.* **128**, 53 (1955).
- [4] M. S. Steinberg, *Science* **137**, 762 (1962).
- [5] J. P. Trinkaus and J. P. Lentz, *Devel. Biol.* **9**, 115 (1964).
- [6] P. B. Armstrong, *Crit. Rev. Biochem. Mol. Biol.* **24**, 119-149 (1989).
- [7] M. S. Steinberg, *Proc. Natl. Acad. Sci. U.S.A.* **48**, 1769 (1962).
- [8] M. S. Steinberg, *J. Exptl. Zool.* **173**, 395 (1970).
- [9] J. Holtfreter, *Arch. Exptl. Zellforsch. Gewebezücht.* **23**, 169 (1939).
- [10] J. P. Trinkaus, *Cells Into Organs: The Forces That Shape The Embryo* (Prentice-Hall, Engelwood Cliffs, NJ, 1984), 2nd ed.
- [11] S. F. Gilbert, *Developmental Biology* (Sinauer Assoc. Inc., Sunderland, MA, 1991).
- [12] *Cell Behavior: Shape, Adhesion and Motility*, edited by J. E. M. Heaysman, C. A. Middleton, and F. M. Watt [*J. Cell Sci. Suppl.* **8** (1987)].
- [13] F. Graner and J. A. Glazier, *Phys. Rev. Lett.* **69**, 2013 (1992).
- [14] J. A. Glazier and F. Graner, *Phys. Rev. E* **47**, 2128 (1993).
- [15] S. A. Newman and W. D. Comper, *Development* **110**, 1 (1990).
- [16] R. Gordon, N. S. Goel, M. S. Steinberg, and L. L. Wiseman, *J. Theoret. Biol.* **37**, 43 (1972).
- [17] H. M. Phillips and M. S. Steinberg, *Proc. Natl. Acad. Sci. U.S.A.* **64**, 121 (1969).
- [18] H. M. Phillips, M. S. Steinberg, and B. Lipton, *Devel. Biol.* **59**, 124 (1977).
- [19] H. M. Phillips and M. S. Steinberg, *J. Cell Sci.* **30**, 1 (1978).
- [20] J. S. Rowlinson and B. Widom, *Molecular Theory of Capillarity* (Clarendon Press, Oxford, 1989).
- [21] J. Folkman and A. Moscona, *Nature (London)* **273**, 345 (1978).
- [22] W. H. Barry and T. W. Smith, *J. Physiol.* **325**, 243 (1982).
- [23] H. M. Phillips and G. S. Davis, *Amer. Zool.* **18**, 81 (1978).
- [24] G. S. Davis, *Amer. Zool.* **24**, 649 (1984).
- [25] E. J. Olson, Undergraduate thesis, Department of Biology, Princeton University, 1980.

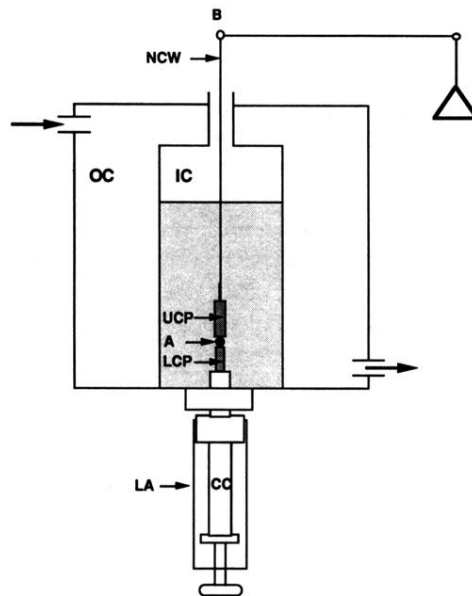


FIG. 1. The parallel plate compression apparatus (not drawn to scale) contains inner and outer Plexiglas chambers. The outer chamber (OC) is connected to a thermostated circulating water pump and serves to maintain the temperature of the inner chamber (IC), which contains tissue culture medium. The lower assembly (LA) screws into the base of the inner chamber, sealing its bottom. The position of its central core (CC), whose tip is the lower compression plate (LCP), can be adjusted vertically to set the distance between the two plates. The upper compression plate (UCP) is a cylinder about 15 mm long suspended from the balance arm (B) by a 0.15 mm diameter nickel-chromium wire (NCW). Its position can be adjusted horizontally to place the upper plate above the aggregate. During an experiment, the cell aggregate (A) is positioned on the lower plate and raised until it contacts the upper plate. Compression of the aggregate reduces the load measured by the balance by an amount equal to the force acting upon the cell aggregate.

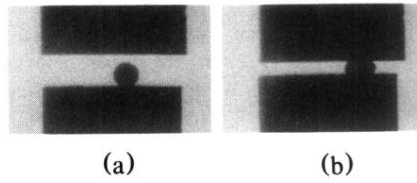


FIG. 2. (a) Spherical liver aggregate on lower compression plate before compression. (b) Same aggregate after initiation of compression.

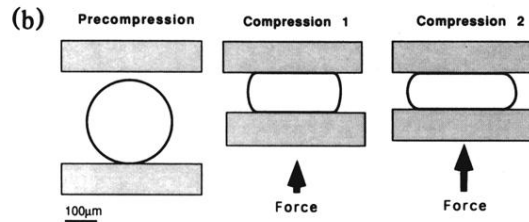
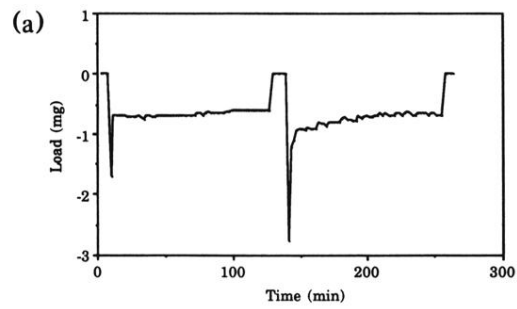


FIG. 3. (a) Force exerted by initially spherical chick liver aggregate 1 (see Table I) upon the upper compression plate (load) as a function of time. After relaxation was complete, the compressing plates were separated and the equilibrium force determined. A second, greater compression was then initiated and the process was repeated. (b) Profile shapes of chick liver aggregate 1, traced using NIH Image are shown before compression was initiated and immediately preceding termination of each compression.

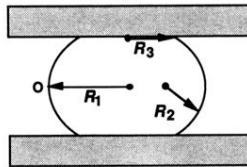


FIG. 4. A liquid droplet compressed between parallel plates to which it does not adhere, at shape equilibrium.  $R_1$  and  $R_2$  are the two primary radii of curvature, respectively, in the plane of and normal to the droplet's axis of symmetry.  $R_3$  is the radius of the droplet's circular area of contact with either compression plate.